Growth and spectroscopic analysis of Tm, Ho:KY F_4

2004 J. Phys.: Condens. Matter 16 241

(http://iopscience.iop.org/0953-8984/16/3/005)

INSTITUTE OF PHYSICS PUBLISHING JOURNAL OF PHYSICS: CONDENSED MATTER

J. Phys.: Condens. Matter **16** (2004) 241–252 PII: S0953-8984(04)69906-1

Growth and spectroscopic analysis of Tm, Ho:KYF_4

Elisa Sani[1], **Alessandra Toncelli, Mauro Tonelli and Francesca Traverso**

NEST-INFM Dipartimento di Fisica, Università di Pisa, via Buonarroti, 2-50127 Pisa, Italy

E-mail: sani@df.unipi.it

Received 3 October 2003
Published 9 January 2004
Online at stacks.iop.org/JPhysCM/16/241 (DOI: 10.1088/0953-8984/16/3/005)

Abstract

Single crystals of lasing Tm, Ho:KYF_4 were successfully grown by the Czochralski method. A complete polarized spectroscopic investigation is given and it is shown that the inhomogeneous broadening of the spectra of rare earth ions can be ascribed to a disordered character of the KYF crystalline structure.

1. Introduction

Tm–Ho lasers are very promising sources in particular for DIAL sensing, LIDAR applications [1, 2] and surgery and the codoping of a fluoride matrix with Tm and Ho has already shown interesting results (see, for example, the broad tunability range obtained in BaY_2F_8 [3]). Laser action has been obtained very recently in Tm–Ho:KYF_4 (potassium–yttrium fluoride, hereafter called KYF) and its tunability range of about 100 nm is, at the present time, the widest ever obtained for thulium and holmium in any crystalline host [4]. To understand the reason for this somewhat unexpected result we decided to carefully investigate the spectroscopic features of Tm–Ho:KYF. In fact, the structure of the crystal is still an open question: KYF has been sometimes considered as a multisite host material [5, 6] and sometimes as a disordered one instead [7, 8]. Moreover previous authors were not in agreement regarding the number of different sites of the trivalent rare earth: despite the fundamental agreement on the existence of two main 'classes' of sites, the number of their 'subclasses' varies, among the various papers, from three for every class [9–11] to two + five [8] and some authors even state [12] that erbium ions occupy only a single class of sites.

2. Structural background

KYF has a trigonal non-centrosymmetric structure derived from the fluorite. The cell parameters are $a = 14.060$ Å, $c = 10.103$ Å and the cations are arranged in an *abc* sequence perpendicular to the c axis [9]. Regarding the ionic positions within the unit cell the works available in the literature are not in agreement: in the first approach [13], the sites of the

[1] Author to whom any correspondence should be addressed.

three cationic layers are assigned to be, in part, occupied by Y^{3+} and, in part, statistically populated either by a Y^{3+} ion or by a K^+ ion. We call the two types of sites first class and second class, respectively. It is possible to show [7] that in the first coordination sphere the two classes of ions are identical (both being surrounded only by fluorine ions) and that in the second coordination sphere ions of the first class are always surrounded by ions of the second class and vice versa. A consequence is that the ions of the first class exist in many different environments because of the statistical character of the Y^{3+}–K^+ second-class-sites occupation. As for the optical features this means that ions in the first class can, in principle, give rise to a large number of different emission spectra according to the effective distribution of Y^{3+} and K^+ in the coordination sphere. The ions of the second class instead are always surrounded by a shell of first-class ions and the differences in their crystalline environment are of a higher order. Thus one can expect from these ions emission spectra with small differences one to another that are most evident at low temperature.

In a second approach [9] the three cationic layers are described as ruled by Y_2F_8 chains alternating with KF_8 chains. In this case, in the yttrium groups there are two different polyhedra YF_7 that share an edge. This structure implies the existence of two types of site, each of them consisting of three subgroups. Then we would expect in this case six different spectra at most.

A considerable amount of spectroscopic work on the KYF crystal has been performed up to now in the visible region, mainly but not only (see [14] on europium and the five papers on erbium from which you can see, for example, [15]) to analyse the upconverted emission in the case of ytterbium codoping: eight papers on Yb–Ho (for example, the latest [16]), one on Yb–Er [17] and one on Yb–Tm [18]. Some works are also available for the UV and VUV regions [7, 19, 20]. The papers devoted to IR spectroscopy are not as many as for the preceding cases: [10] on holmium, [21] on erbium and finally [5] and [8] on neodymium. Among all these works, very few of them are really oriented for understanding the structural characteristics of the crystal (see [7, 8] and [10]) and, as already said, these are not in agreement in their conclusions.

In this framework we try to give some hints about the structure of the KYF matrix, analysing the features of the optical spectra mainly of thulium in a Tm–Ho codoped sample cut from the same boule as the lasing sample of [4]. In this way we hope to explain the reason for the obtained wide tunability of the KYF laser.

3. Growth and spectroscopy apparatus

The growth apparatus consists of a home-made computer-controlled Czochralski furnace with a resistive heater. Crystal growth is carried out in an inert argon atmosphere at temperatures around 805 °C. The high-purity growth powders (from *AC Materials*, Orlando, FL) are suitably mixed, according to the non-congruently melting characteristics of the crystal [22]. Preliminary growth runs are performed in order to obtain a KYF undoped single crystal for high quality oriented seeds. Then the 5.2% thulium and 0.5% holmium nominal doping is obtained by adding the proper amounts of TmF_3 and HoF_3 to the KF–YF_3 powder[2]. In all cases the growth rate was 0.5 mm h^{-1} and the rotation rate 7 RPM.

The average size of the obtained Tm, Ho:KYF single crystal was about 17 mm in diameter and 62 mm in length and its mass was about 21 g.

The crystal was oriented by the x-ray backscattering Laue technique and cut with the *c* axis parallel to the polished faces in order to investigate its polarization-dependent optical properties.

[2] The indicated concentrations are given in % Tm or Y sites and refer to the melt composition.

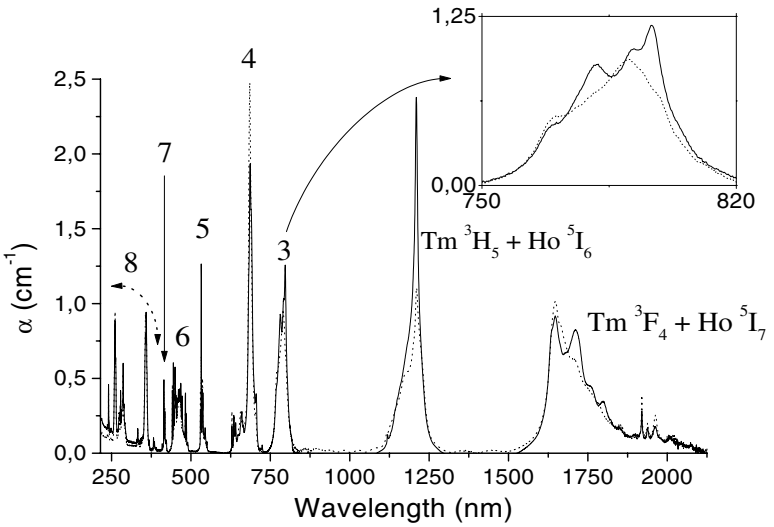

Figure 1. Polarized absorption spectra at room temperature. In the inset is shown the diode-pumping region. The full curve refers to **E** ∥ **c** polarization, whereas the dotted curve refers to **E** ⊥ **c** polarization. The numbered groups of peaks refer to the following transitions: (3) thulium $^3H_4$ superimposed on holmium $^5I_4$; (4) thulium $^3F_3 + {}^3F_2$ superimposed on holmium $^5F_5$; (5) holmium $^5S_2 + {}^5F_4$; (6) thulium $^1G_4$ superimposed on holmium from $^5F_3$ to $^5F_1$; (7) holmium $^5G_5$; (8) thulium from $^1D_2$ to $^3P_2$ superimposed on holmium from $^1G_4$ to $^3H_4$.

Polarized absorption measurements at room temperature were performed by a Cary 500 Spectrophotometer with a resolution of 0.6 nm up to 820 nm and 1.5 nm beyond that.

The excitation source for recording the 10, 77 K and room temperature fluorescence spectra was a cw tunable Ti:Al_2O_3 laser that pumped the 800 nm band of thulium. The luminescence was mechanically chopped and focused on the input slit of a monochromator having a 25 cm focal length, equipped with a 300 lines mm^{-1} grating for the 2 μm fluorescence detection and with a 1200 lines mm^{-1} grating for the 800 nm measurements. The signal was detected by a cooled InSb detector in the 2 μm wavelength region and by a Hamamatsu R316 photomultiplier around 800 nm, fed into a preamplifier and processed by a lock-in standard set-up. The resolution of the 2 μm fluorescence spectra was 0.5 nm at 10 K and 0.7 nm at room temperature, whereas the resolution of the 800 nm spectra was 0.2 nm.

The source used in the fluorescence lifetime measurements was a pulsed tunable Ti:Al_2O_3 laser with 10 Hz repetition rate and 20 ns pulse width. The maximum pulse energy was reduced as much as possible in order to minimize non-linear power-dependent effects. The signal was detected by the same experimental apparatus described above, but the signal from the detector was sent, by a fast amplifier, to a digital oscilloscope connected to a computer. The response time of the system was about 1 μs.

Excitation spectra were recorded using the same experimental set-up employed in the 2 μm fluorescence measurements. The resolution of these spectra was 0.1 nm.

4. Spectroscopic analysis and decay kinetics

We recorded the room-temperature polarized absorption spectra (**E** ∥ **c** and **E** ⊥ **c**) from the UV up to the IR wavelength regions (figure 1). The spectra did not show any spurious bands due to hydroxyl radicals or other unwanted impurities within the sensitivity of our Cary 500

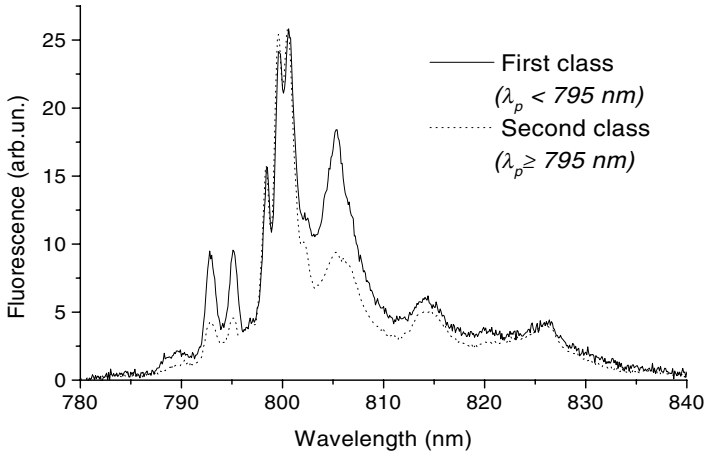

Figure 2. The two classes of 77 K thulium emission spectra (**E** ∥ **c** polarization).

Spectrophotometer. Indicative assignments of the bands are made in the caption of the figure: one can see that no contaminant absorption is present. All the bands appear considerably broadened according to the existence of multiple sites for the rare-earth ion. The inset of figure 1 shows the 800 nm band, which can be attributed to the thulium $^3H_6 \rightarrow {}^3H_4$ optical transition superimposed on the holmium $^5I_8 \rightarrow {}^5I_4$. These spectra, which are interesting for diode pumping, are peaked at 796.5 nm ($\alpha = 1.2\ \mathrm{cm}^{-1}$) in the polarization **E** ∥ **c** and at 790.2 nm ($\alpha = 0.9\ \mathrm{cm}^{-1}$) for **E** ⊥ **c**. The FWHM of the band is about 30 nm: a feature which appears particularly appealing because it reduces the demands on the diode laser temperature control. The 1.7 μm region is important both as an evaluation of an alternative pumping channel [23] and as a quantitative check of the reabsorption of the holmium fluorescence light. The absorption spectra in this region are shown in figure 1: the maximum feature is a large peak at 1648 nm ($\alpha = 1\ \mathrm{cm}^{-1}$) in **E** ⊥ **c** polarization, whereas the maximum of the holmium absorption lies at 1920 nm and its value is $\alpha = 0.4\ \mathrm{cm}^{-1}$ in the same polarization (figure 1).

The excitation spectra of the 2 μm holmium transition have been acquired at 10 K in **E** ∥ **c** polarization for two observation wavelengths (2075 and 2103 nm) and scanning the 764–800 nm region. The two recorded spectra are identical and this shows that the holmium loses memory of the pump wavelength. The short-wavelength side (764–790 nm) shows some broad peaks emerging from a non-zero background that could probably be due to the envelope of many unresolved peaks. For longer wavelengths a series of very narrow lines appears.

Because of the fact that this spectrum is rich in lines and each line could, in principle, show one different excitation channel of thulium, we observed the 800 nm $^3H_4 \rightarrow {}^3H_6$ emission of thulium and the 2 μm $^5I_7 \rightarrow {}^5I_8$ transition of holmium. Both transitions have been observed at two different temperatures, namely 77 and 10 K. The analysis of these spectra can help us to understand the morphological characteristics of the host matrix.

At 77 K the spectra of thulium transitions have been acquired in the **E** ∥ **c** polarization for nine laser excitation wavelengths, ranging from 768 to 798.2 nm. By observing the experimental results we found spectra with two different shapes for pump wavelengths shorter or longer than 795 nm. We called the two kinds of spectra first and second class, respectively, as shown in figure 2.

In the first class (pumped between 768 and 795 nm) we found four spectra that differ from each other regarding the relative height of the three main peaks at 794.4, 800 and 804.6 nm.

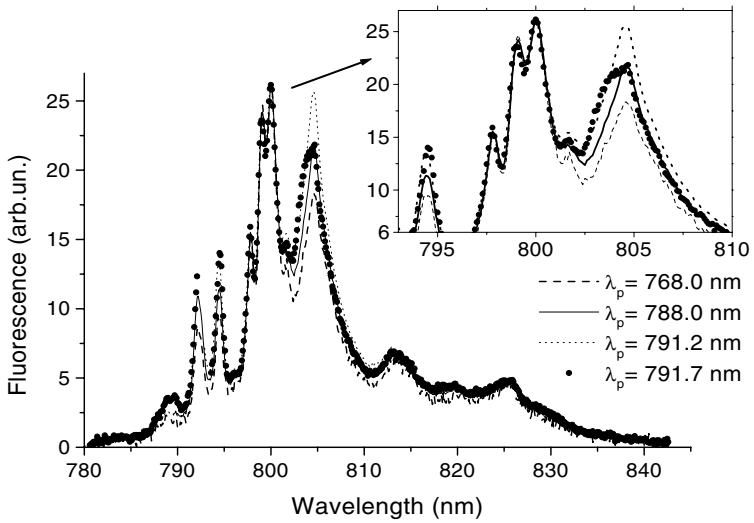

Figure 3. Detail of the first-class 77 K **E** ∥ **c** emission spectra.

Figure 3 shows this group of spectra normalized one to the other with respect to the 800 nm emission peak. In contrast the spectra recorded after excitation at wavelengths longer or equal to 795 nm (second class) are identical.

We also analysed the same thulium transition at 10 K temperature for two different polarizations **E** ∥ **c** and **E** ⊥ **c**, respectively. The excitation wavelengths are the same as in the 77 K measurements plus one extra (776.1 nm). The spectra are quite different from one another and from a qualitative look we can see in both polarizations the gross division into the two classes already shown by the 77 K measurements. In fact, for the **E** ∥ **c** polarization and exciting the sample with wavelengths shorter than 795 nm, we found a high unresolved peak, which is located between 800 and 805 nm, and many narrow peaks in the short wavelength side of the spectra (as shown in the lower part of figure 4). If instead we excite the crystal with wavelengths longer or equal to 795 nm the maximum feature previously described becomes much less intense and is shifted to longer wavelengths and the number of peaks is reduced, as shown in the upper part of figure 4. As a result of this investigation the 10 K temperature spectra can be divided into the same two classes as in the 77 K case, but in this case the spectra are better resolved and the two classes can be further divided into subclasses.

The same qualitative investigation can be performed in **E** ⊥ **c** polarization and figure 5 shows our results: the 795 nm pump wavelength divides the spectra into two classes. For pumping at shorter wavelengths one can find a recursive structure of four peaks of increasing intensity and maximum at about 802 nm. Moreover, all these spectra show an emission peak at 795 nm and, in three cases, some peaks at lower emission wavelengths. This four-peak structure has a completely different shape for excitation wavelengths longer or equal to 795 nm: in particular, the intensities are no longer increasing with the wavelength. Besides, in these last cases both the narrow peak and the broad peak regions are less extended in wavelength (from 796 to 802 nm and from 802 to 830 nm, respectively).

Another series of fluorescence spectra at four different excitations (776.1, 788, 791.2 and 795.3 nm) has been acquired at 10 K in the 1980–2140 nm wavelength region of the holmium $^5I_7 \rightarrow {}^5I_8$ emission and these spectra appear identical to one another. The reason for the holmium emission insensitivity to the pump wavelength will be discussed in the next section.

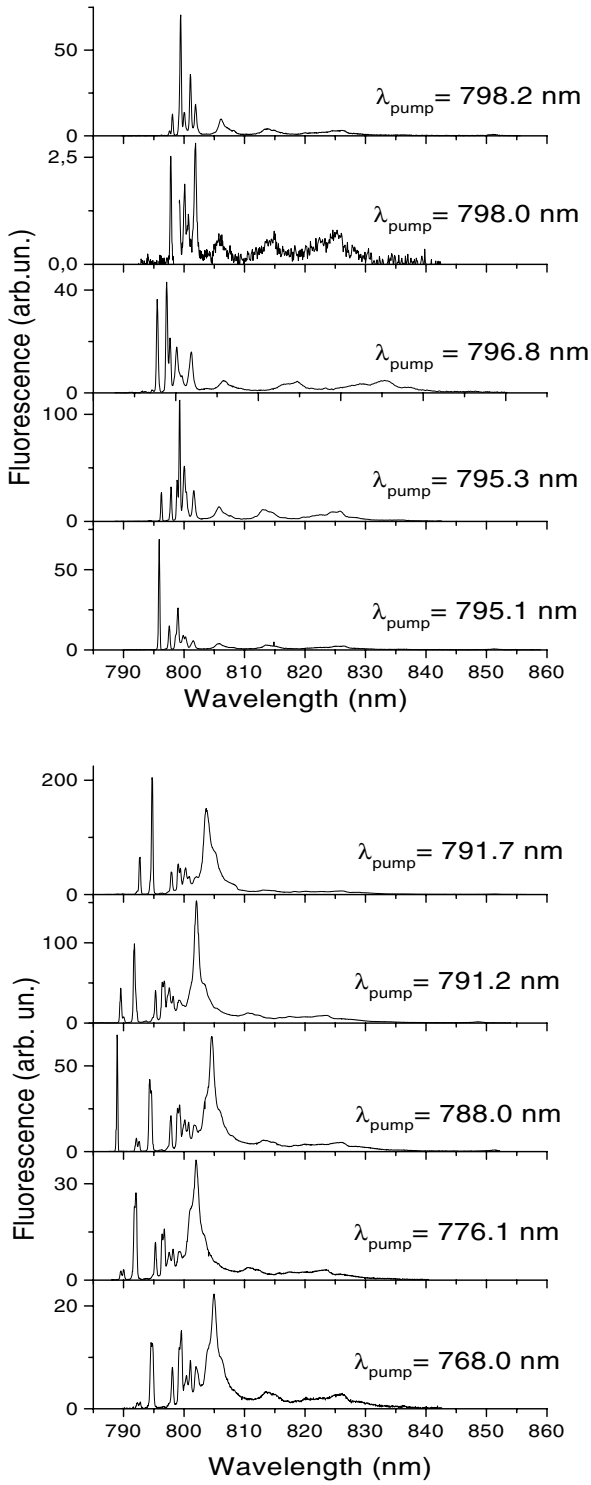

Figure 4. Thulium emission spectra **E** ∥ **c** at 10 K temperature. Lower part: first class. Upper part: second class.

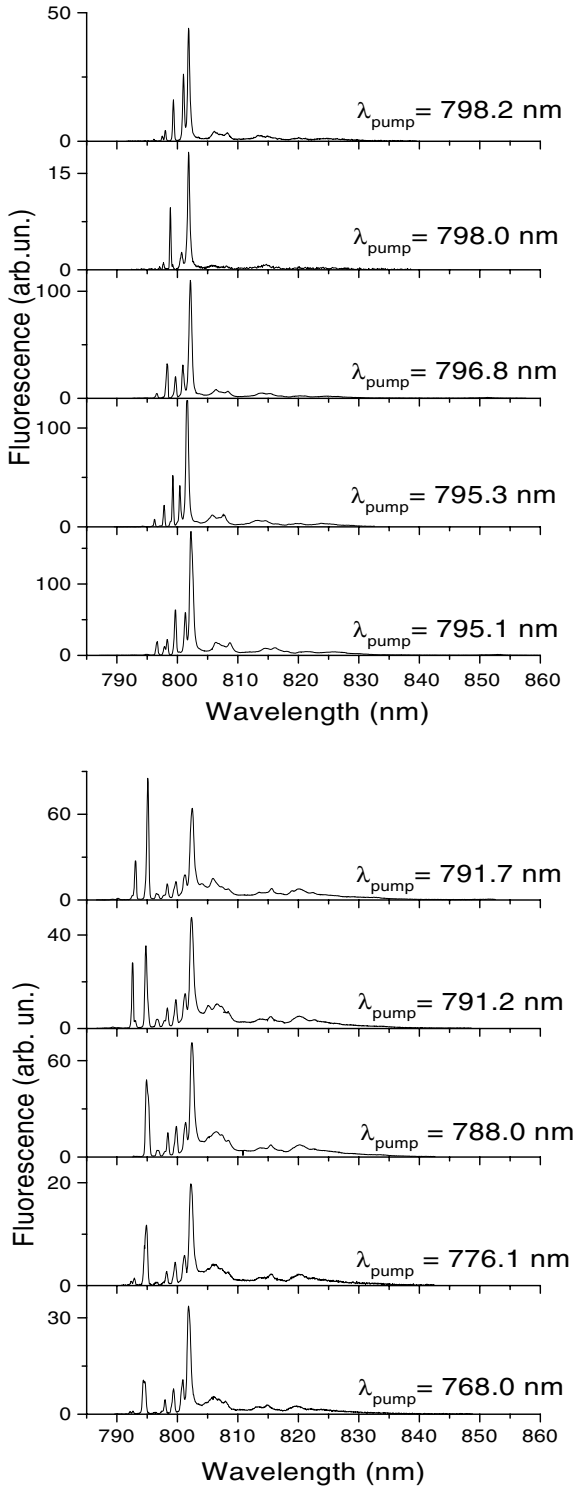

Figure 5. Thulium emission spectra $\mathbf{E} \perp \mathbf{c}$ at 10 K temperature. Lower part: first class. Upper part: second class.

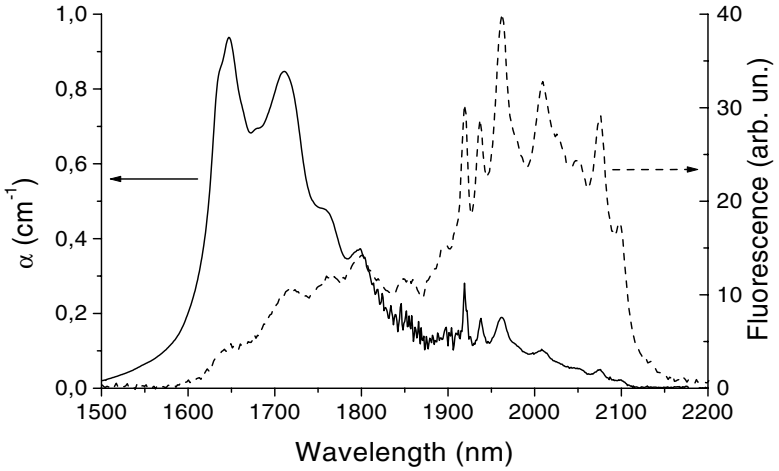

Figure 6. **E** ∥ **c** absorption and emission spectra at room temperature. In absorption the main peaks are the ones from thulium whereas in emission the holmium $^5I_7 \rightarrow {}^5I_8$ peaks are very intense despite the much lower holmium doping level.

To fully characterize the spectral features of interest for laser emission, we also acquired the polarized fluorescence spectra in the 2 μm region at room temperature. At this temperature the emissions of thulium and holmium overlap: from a comparison between the 10 K and room temperature emission spectra and the room temperature absorption ones we could attribute to holmium only the peaks at wavelengths longer than 1950 nm. In figure 6 we show together the **E** ∥ **c** room temperature absorption and emission spectra. This shows the possibility of obtaining the tunability of a 2 μm Tm–Ho:KYF laser wider than 200 nm because of the small reabsorption losses in this wavelength region. Actually in [4] a tunability of 99 nm has already been obtained, but in that case the tunability range was limited by the optics.

We recorded the decay times of the $^5I_7$ level of holmium as a function of the temperature of the sample from 10 to 298 K for excitation at 795 nm. The lifetime remains constant within the experimental errors and the room temperature value is 21 ± 2 ms, in agreement with that reported in [16].

Finally we measured the lifetime of various peaks of the thulium $^3H_4$ level. We chose 10 K crystal temperature and five different pump wavelengths (768, 776.1, 791.2, 795.3 and 798.2 nm) and some emission peaks (typically one narrow peak located around 795 or 800 nm and two wider peaks: one at about 805 nm and the other at longer wavelengths). The peaks are chosen from the **E** ∥ **c** emission polarization and, to improve the selectivity with respect to the detected fluorescence, we set the slits of the monochromator to have a resolution of 0.3 nm. All the decays are non-exponential due to thulium cross-relaxation and energy transfer to holmium processes, but the initial non-exponential behaviour is different between the different decays (figure 7), giving evidence in this way of a difference between the energy transfer processes of the individual sites (although difficult to evaluate from a quantitative point of view). In particular, if we fix the excitation and we look at the initial times of the decays, the fastest decay is always that relative to the shortest-wavelength observation peak and the slowest the one relative to the longest-wavelength detection. Least-squares fits, performed with an exponential function on the tail of the decays, have shown that, for a fixed pump wavelength, the various peaks had the same lifetime within experimental errors. This confirms the fundamental similarity of the various peaks, at fixed excitation, as belonging to the same

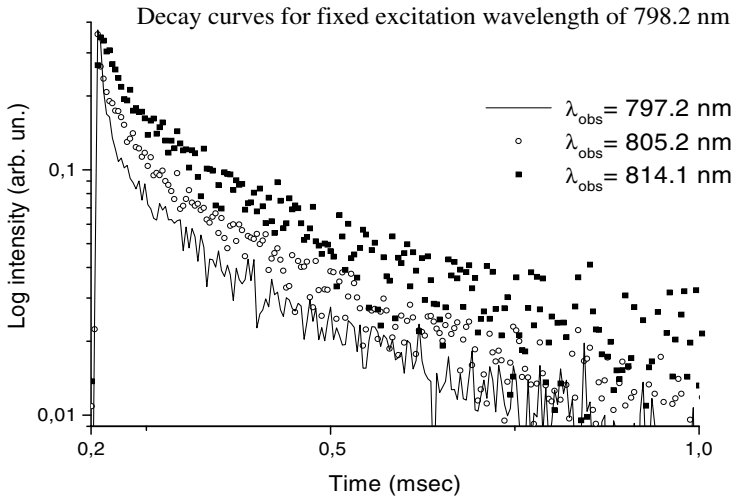

Figure 7. Thulium lifetimes at 10 K temperature for fixed excitation wavelength and as a function of the observation wavelength.

Table 1. Lifetimes of the $^3H_4$ level of thulium at 10 K temperature.

λ_{exc} (nm)	Lifetime (μs)
768.0	260 ± 10
776.0	310 ± 10
791.3	340 ± 20
795.3	330 ± 10
798.2	340 ± 20

class. The mean values of the lifetime for every excitation wavelength are shown in table 1. Even if the experimental errors did not show any difference (if present) between the lifetimes for the last three laser wavelengths, the behaviour of the lifetimes with respect to the two shortest pump wavelengths compared to the remaining ones could be interpreted as a hint of a lengthening of the decay as the excitation is shifted to lower energies, although additional investigations would be needed to draw a clear conclusion.

5. Discussion

The results of the fluorescence measurements at temperatures of 77 and 10 K clearly show the two classes of sites found by previous authors. The pumping wavelength that selects one type of site or another is between 791.7 and 795 nm, even though in the following we will refer to 795 nm for clarity. As already said, we call 'first class' the spectra obtained for excitation wavelengths shorter than 795 nm and 'second class' the wavelengths obtained after excitation equal to or above 795 nm. At 77 K temperature the two classes are clearly different (figure 2), but the emission lines are thermally broadened and all the spectra of the second class are identical whereas we can distinguish at least four different spectra in the first class (figure 3). At 10 K crystal temperature the lines are well separated so even in the second class we can identify individual spectra as a function of the laser wavelength. For each class of sites we can distinguish at least five different spectra (figures 4 and 5). Our results agree with those in [7] and [8].

Let us now briefly recall the implications of the two hypotheses about the structure of KYF:

- The first approach ('disordered' theory):
  - (i) some positions of the cations are statistically populated by yttrium or potassium;
  - (ii) the first-class sites are the ones occupied strictly by Y^{3+}, while the second-class ones are statistically populated either by a Y^{3+} or by a K^{+};
  - (iii) in the second coordination sphere every ion is surrounded by ions of the opposite class;
  - (iv) every class consists of many subclasses, but the number of subclasses is in principle unknown;
  - (v) the differences among the spectra produced by ions of the first class are more evident than the ones among the spectra produced by the other class.
- The second approach ('multisite' theory):
  - (i) the positions of the cations are strictly determined within the cell;
  - (ii) there are two different polyhedra YF_7 and therefore two different classes of RE^{3+} sites;
  - (iii) every class of sites consists of three subclasses.

Our measurements are well explained in the framework of the first approach, if we consider that laser wavelengths above or below 795 nm selectively excite only sites of the second or of the first class, respectively. If we count the peaks of the two kinds of spectra we can see that the spectra of the first class always show more lines than the those of the second class: this means that in the second class the number of different sites is higher. Moreover the fact that, at 77 K temperature, all the second-class pump wavelengths produced identical spectra whereas for the first class we obtained different spectra means that only the differences between the first-class spectra could survive to the thermal broadening, i.e. the differences in the first-class fluorescence are larger than those in the second class.

These facts allow us to attribute the first or the second class of spectra to the first or the second class of sites, respectively. Another argument that agrees with this attribution is the larger crystal splitting shown by the first class of spectra. In fact, it was demonstrated in [8] that the splitting is larger for ions in the first class of sites. We emphasize that our measurements have been performed both at 10 and 77 K crystal temperature, whereas the results of [10] refer only to 80 K temperature. The only low temperature spectral analysis available in the literature is the one of [8] on Nd doping and in this case the authors found more than six types of sites.

Apart from the thermal effects, another reason for the disagreement between the number of sites reported in the literature could be the growth technique of the samples employed. In fact, in the case of YAG growth, the features of the dopant site in the crystal have been shown to vary for different growth methods [24]. Our Czochralski furnace is very similar to that of Jenssen [8], whereas Chai used a TSSG technique in all his growths (see, for example, [22]) and Khaidukov [11, 14] grew by hydrothermal synthesis. Regarding the structural papers, the samples of [9] and [12] have been supplied by this latter grower, whereas the samples of [13] have been grown by the Bridgman technique [25].

The results summarized up to this point have been derived by the analysis of thulium spectra. Because of the fact that our crystal has been grown for laser applications, we were more interested in evaluating the optical features of holmium, which is the active ion for 2 μm laser emission: we observed an absolute identity of the Ho^{3+} emission spectra by varying the excitation wavelengths even at 10 K and a similar behaviour of the 10 K holmium excitation spectra as a function of the observation wavelength.

In order to explain this result we must keep in mind that the number of different sites is helpful with respect to energy transfers because it increases the number of possible resonances. In fact, because of the high number of subsites, we can have a quasi-continuous distribution of their individual splittings and so, in principle, a thulium ion in a well determined site can cross-relax with another thulium ion in a different environment and both can transfer to holmium. In this way the selective excitation of the $^3H_4$ level of thulium become less selective (or even, in the limit case, non-selective) when transformed in $^3F_4$ excitation and so the holmium emission loses memory about any site-selective excitation. In fact, a KYF crystal has already been found a very favourable host for energy transfers (see, for example, [22, 26, 27]).

6. Conclusions

In this work a KYF single crystal doped with 5.2% Tm^{3+} and 0.5% Ho^{3+} has been characterized by room temperature absorption and by low temperature emission spectroscopy in order to explain the wide tunability range already obtained in a Tm–Ho:KYF laser [4]. Moreover, by comparing the room temperature absorption and emission spectra in the 2 μm wavelength region, we show the possibility for an even wider tunability range. By analysing the 800 nm thulium emission we found two classes of sites, with equal numbers of subclasses. By time-resolved emission spectroscopy we showed at short times a different energy transfer dynamics between the various sites. By recording the holmium emission and its low temperature excitation spectra we could infer the no-memory characteristics of the holmium excitation. Regarding the open question of the structure of KYF, which has been the first aim of our measurements, the present work confirms the hypothesis of a statistical distribution of Y^{3+} sites versus the multisite one.

Acknowledgments

The authors wish to thank Ilaria Grassini for skill and competence in preparing the samples and A Cassanho and H P Jenssen for helpful discussions. One of the authors (ES) is supported by a grant from Alcatel Italia.

References

[1] Murray K E, Barnes N P, Walsh B M, Hutcheson R L and Kotka M K 2000 *Advanced Solid State Lasers* (*OSA Trends in Optics and Photonics* vol 34) ed H Injeyan, U Keller and C Marshall (Washington, DC: Optical Society of America) p 170

[2] Henderson S W, Hale C P, Magee J R, Kavaja M J and Huffeker A V 1991 *Opt. Lett.* **16** 773

[3] Cornacchia F, Sani E, Toncelli A, Tonelli M, Marano M, Taccheo S, Galzerano G and Laporta P 2002 Optical spectroscopy and diode-pumped laser characteristics of codoped Tm–Ho:YLF and Tm–Ho:BaYF: a comparative analysis *Appl. Phys.* B **75** 817–22

[4] Galzerano G, Sani E, Toncelli A, Taccheo S, Tonelli M and Laporta P 2003 2 μm widely-tunable CW diode-pumped Tm–Ho:KYF_4 laser *Opt. Lett.* at press

[5] Allik T A, Merckle L D, Utano R A, Chai B H T, Lefaucheur J-L V, Voss H and Dixon G J 1993 Crystal growth, spectroscopy and laser performance of Nd^{3+}:KYF_4 *J. Opt. Soc. Am.* B **10** 633–7

[6] Zhang X X, Hong P, Bass M and Chai B H T 1995 Multisite nature and efficient lasing at 1041 and 1302 nm in Nd^{3+} doped potassium yttrium fluoride *Appl. Phys. Lett.* **66** 926–8

[7] Sytsma J, Kroes S J, Blasse G and Khaidukov N M 1991 Spectroscopy of Gd^{3+} in KYF_4: a system with several luminescent sites *J. Phys.: Condens. Matter* **3** 8959–66

[8] Yamaguchi Y, Dinndorf K M, Jenssen H P and Cassanho A 1993 Spectroscopy of Nd:KYF_4 *OSA Proc. Adv. Solid State Lasers* **15** 36–40

[9] Le Fur Y, Khaidukov N M and Aléonard S 1992 Structure of KYF_4 *Acta Crystallogr.* C **48** 978–82

[10] Peale R E, Weidner H, Summers P L and Chai B H T 1994 Site-selective spectroscopy of Ho^{3+}:KYF_4 *J. Appl. Phys.* **75** 502–6
[11] Bouffard M, Duvaut T, Jouart J P, Khaidukov N M and Joubert M F 1999 Site-selective upconversion excitation of Er^{3+}:KYF_4 *J. Phys.: Condens. Matter* **11** 4775–82
[12] Le Fur Y, Khaidukov N M and Aléonard S 1992 Structure of $KY_{0.95}Er_{0.05}F_4$ *Acta Crystallogr.* C **48** 2062–4
[13] Aleonard S, Le Fur Y, Pontonnier L, Gorius M F and Roux M-Th 1978 Quelques fluorures mixtes terre rare-metal alcalin de structures derivées de celle de la fluorine *Ann. Chim. Fr.* **3** 417–27
[14] Khaidukov N M, Zhang X X and Jouart J-P 1997 Photoluminescence of Eu^{3+} in KYF_4 and $KLuF_4$ *J. Lumin.* **72–74** 213–4
[15] Brede R, Heumann E, Koetke J, Danger T, Huber G and Chai B 1993 Green upconversion laser emission in Er-doped crystals at room temperature *Appl. Phys. Lett.* **63** 2030–1
[16] Möbert P E-A, Diening A, Heumann E, Huber G and Chai B H T 1998 Room-temperature continuous-wave upconversion-pumped laser emission in Ho, Yb:KYF_4 at 756, 1070, and 1390 nm *Laser Phys.* **8** 210–3
[17] Caro P and Porcher P 1979 Infra-red excitation of visible luminescence in up-converters rare earth materials *J. Lumin.* **18/19** 257–61
[18] Zhang X X, Hong P, Bass M and Chai B H T 1995 Blue upconversion with excitation into Tm ions at 780 nm in Yb- and Tm-codoped fluoride crystals *Phys. Rev.* B **51** 9298–301
[19] Khaidukov N M, Kirm M, Lam S K, Lo D, Makhov V N and Zimmerer G 2000 VUV spectroscopy of KYF_4 crystals doped with Nd^{3+}, Er^{3+} and Tm^{3+} *Opt. Commun.* **184** 183–93
[20] Kaminskii A A, Mironov A S, Bagaev S N, Boulon G and Djeu N 1994 Strong ultraviolet and visible radiative channels of Nd^{3+}-doped insulating fluoride crystals *Phys. Status Solidi* b **195** 487–504
[21] Shmaul B, Zhang X X, Villaverde A B, Bass M, Pham A and Chai B H T 1993 Spectroscopy and lasing performance of Er-doped $LiYF_4$ and KYF_4 *Proc. SPIE* **1863** 138–44
[22] Chai B, Lefaucheur J, Pham A, Lutts G and Nicholls J 1993 Growth of high-quality single crystals of KYF_4 by TSSG method *Proc. SPIE* **1863** 131–5
[23] Cornacchia F, Di Lieto A, Maroni P, Minguzzi P, Toncelli A, Tonelli M, Sorokin E and Sorokina I 2001 A cw room-temperature Ho,Tm:YLF laser pumped at 1.682 μm *Appl. Phys.* B **73** 191–4
[24] Lupei V, Lupei A, Tiseanu C, Georgescu S, Stoicescu C and Nanau P M 1995 High-resolution optical spectroscopy of YAG:Nd: a test for structural and distribution models *Phys. Rev.* B **51** 8–17
[25] Marie-France G 2002 private communication
[26] Zhang X X, Bass M, Chai B H T and Peale R E 1993 Comparison of Yb, Ho upconversion energy transfer in different fluoride crystals *OSA Proc. Advanced Solid-State Lasers* vol 15, ed A A Pinto and T Y Fan (Washington, DC: Optical Society of America) pp 253–7
[27] Peale R E, Weidner H, Summers P L, Zhang X X, Bass M and Chai B H T 1993 Comparative Fourier spectroscopy of Ho^{3+} and Yb^{3+} in KYF_4, BaY_2F_8 and $LiYF_4$ *OSA Proc. Advanced Solid-State Lasers* vol 15, ed A A Pinto and T Y Fan (Washington, DC: Optical Society of America) pp 450–3